

1-1-2021

Unexpected role of communities colonizing dead coral substrate in the calcification of coral reefs

Manoela Romanó de Orte
Carnegie Institution of Washington

David A. Kowweek
Carnegie Institution of Washington

Tyler Cyronak
Nova Southeastern University, tcyronak@nova.edu

Yuichiro Takeshita
Monterey Bay Aquarium Research Institute

Alyssa Griffin
Scripps Institution of Oceanography

See next page for additional authors

Find out more information about [Nova Southeastern University](#) and the [Halmos College of Natural Sciences and Oceanography](#).

Follow this and additional works at: https://nsuworks.nova.edu/occ_facarticles

 Part of the [Marine Biology Commons](#), and the [Oceanography and Atmospheric Sciences and Meteorology Commons](#)

NSUWorks Citation

Manoela Romanó de Orte, David A. Kowweek, Tyler Cyronak, Yuichiro Takeshita, Alyssa Griffin, Kennedy Wolfe, Alina Szmant, Robert Whitehead, Rebecca Albright, and Ken Caldeira. 2021. Unexpected role of communities colonizing dead coral substrate in the calcification of coral reefs .*Limnology and Oceanography* . https://nsuworks.nova.edu/occ_facarticles/1161.

This Article is brought to you for free and open access by the Department of Marine and Environmental Sciences at NSUWorks. It has been accepted for inclusion in Marine & Environmental Sciences Faculty Articles by an authorized administrator of NSUWorks. For more information, please contact nsuworks@nova.edu.

Authors

Kennedy Wolfe

The University of Queensland

Alina Szmant

University of North Carolina Wilmington

Robert Whitehead

University of North Carolina Wilmington

Rebecca Albright

California Academy of Sciences

Ken Caldeira

Carnegie Institution of Washington

Unexpected role of communities colonizing dead coral substrate in the calcification of coral reefs

Manoela Romanó de Orte ^{1,*} David A. Koweek ^{1,a} Tyler Cyronak ² Yuichiro Takeshita ³
Alyssa Griffin ^{4,5} Kennedy Wolfe ⁶ Alina Szmant,⁷ Robert Whitehead,⁷ Rebecca Albright,⁸
Ken Caldeira ^{1,9}

¹Department of Global Ecology, Carnegie Institution for Science, Stanford, California

²Department of Marine and Environmental Sciences, Nova Southeastern University, Dania Beach, Florida

³Monterey Bay Aquarium Research Institute, Moss Landing, California

⁴Scripps Institution of Oceanography, La Jolla, California

⁵Bodega Marine Laboratory, University of California, Davis, Bodega Bay, California

⁶Marine Spatial Ecology Lab, University of Queensland, St. Lucia, Queensland, Australia

⁷Center for Marine Science, University of North Carolina Wilmington, Wilmington, North Carolina

⁸California Academy of Sciences, San Francisco, California

⁹Breakthrough Energy, Kirkland, Washington

Abstract

Global and local anthropogenic stressors such as climate change, acidification, overfishing, and pollution are expected to shift the benthic community composition of coral reefs from dominance by calcifying organisms to dominance by non-calcifying algae. These changes could reduce the ability of coral reef ecosystems to maintain positive net calcium carbonate accretion. However, relationships between community composition and calcification rates remain unclear. We performed field experiments to quantify the metabolic rates of the two most dominant coral reef substrate types, live coral and dead coral substrate colonized by a mixed algal assemblage, using a novel underwater respirometer. Our results revealed that calcification rates in the daytime were similar for the live coral and dead coral substrate communities. However, in the dark, while live corals continued to calcify at slower rates, the dead coral substrate communities exhibited carbonate dissolution. Daytime net photosynthesis of the dead coral substrate communities was up to five times as much as for live corals, which we hypothesize may have created favorable conditions for the precipitation of carbonate minerals. We conclude that: (1) calcification from dead coral substrate communities can contribute to coral reef community calcification during the day, and (2) dead coral substrate communities can also contribute to carbonate mineral dissolution at night, decreasing ecosystem calcification over a diel cycle. This provides evidence that reefs could shift from slow, long-term accretion of calcium carbonate to a state where large daily cycling of calcium carbonate occurs, but with little or no long-term accumulation of the carbonate minerals needed to sustain the reef against erosional forces.

Introduction

Coral reefs worldwide are suffering substantial declines in coral cover and species diversity. Across the Caribbean, coral cover declined from about 50% to about 10% between the 1970s and the 2000s, while in the Indo-Pacific region, it declined from 42.5% to 22.1% between the early 1980s and 2000s (Gardner et al. 2003; Bruno and Selig 2007). These losses are attributed to a combination of global and local stressors, including disease outbreaks, overfishing, sedimentation, and climate change. As coral reefs degrade, benthic community composition undergoes phase-shifts from dominance by calcifying organisms such as corals and crustose coralline algae to dominance by turf algae and fleshy macroalgae (Hughes et al. 2007; Graham et al. 2015; Clements et al.

*Correspondence: mromano@carnegiescience.edu

This is an open access article under the terms of the Creative Commons Attribution License, which permits use, distribution and reproduction in any medium, provided the original work is properly cited.

Additional Supporting Information may be found in the online version of this article.

^aPresent address: Ocean Visions, Inc., 225 Baker Street, Atlanta, GA 30313, USA

Author Contribution Statement: A.S. and R.W. designed CISME. M.R.O., K.C. and Y.T. designed field experiments. M.R.O., K.C. and K.W. conducted field measurements. M.R.O., A.G., T.C., Y.T. and K.W. analyzed samples. M.R.O. and D.A.K. analyzed data. M.R.O. wrote original draft. All co-authors revised manuscript.

2018). These shifts can have significant impacts on coral reef metabolism and reef carbonate chemistry dynamics (Kinsey, 1985; Page et al. 2017). In combination with decreases in calcification due to ocean acidification (Albright et al. 2018), shifts in community composition could reduce the ability of coral reef ecosystems to maintain positive net calcium carbonate (CaCO_3) accretion. Net CaCO_3 accretion is the balance between production of carbonate minerals through biologically mediated calcification, and loss of these minerals through physical erosion and chemical dissolution. However, relationships between recent shifts in community composition and estimates of net calcification based on geochemical anomalies measured in seawater are still unclear.

It is often assumed that decreases in coral cover will lead to decreases in net ecosystem calcification (gross calcification minus dissolution), mainly due to the well-established connection between corals and CaCO_3 production rates (Kinsey 1985). Some field-based observations following coral bleaching events have demonstrated concurrent changes between ecosystem calcification and coral cover. However, causal relationships remain unclear (Courtney and Andersson 2019). For instance, bleaching and cyclones in the northern section of Australia's Great Barrier Reef caused coral cover to decline from 8.3% pre-disturbance to 2.6% post-disturbance, and ecosystem calcification to decline from $61 \pm 12 \text{ mmol CaCO}_3 \text{ m}^{-2} \text{ d}^{-1}$ pre-disturbance to $32 \pm 10.8 \text{ mmol CaCO}_3 \text{ m}^{-2} \text{ d}^{-1}$ post-disturbance (McMahon et al. 2019). However, Kayanne et al. (2005) measured varying ecosystem calcification responses of reefs in Palau and Japan to bleaching events. In Palau, the bleaching event decreased coral cover from 8.1% pre-bleaching to 1.3% post-bleaching and decreased ecosystem calcification from $130 \text{ mmol CaCO}_3 \text{ m}^{-2} \text{ d}^{-1}$ pre-bleaching to $74 \text{ mmol CaCO}_3 \text{ m}^{-2} \text{ d}^{-1}$ post-bleaching. In contrast, calcification remained steady in Japan during the bleaching event whereas coral cover was reduced from 7.1% to 5.8% in 4 months. Finally, (DeCarlo et al. 2017) showed no relationship between coral cover and ecosystem calcification in the South China Sea and reported high calcification rates despite relatively high densities of fleshy macroalgae.

Community-scale estimates of net calcification and net primary production (i.e., photosynthesis minus respiration) based on chemical anomalies measured in bulk seawater (e.g., total alkalinity, dissolved inorganic carbon, dissolved oxygen) cannot be disaggregated to determine the relative contribution of each benthic group to a coral reef's overall metabolic signal. It is often assumed that ecosystem calcification is related to "traditional calcifiers" such as corals and crustose coralline algae. This approach ignores the potential roles of other benthic substrates such as the algal turf community and carbonate sediments. While the role of CaCO_3 sediments in reef biogeochemistry has received recent attention (Cyronak et al. 2013; Eyre et al. 2018), it is unclear what role other components of coral ecosystems play in ecosystem

calcification. This lack of attention to nontraditional calcifiers is surprising given that, for instance, algal turfs can comprise 30–50% of the coral reef benthic community (Harris 2015). Algal assemblages are usually the first colonizers of bare CaCO_3 substrate and, therefore, are becoming more abundant in coral reef ecosystems as bleaching becomes more frequent and intense and reefs degrade (Rogers and Miller 2006; Hughes et al. 2007; Swierts and Vermeij 2016). On top of ocean warming, other anthropogenic pressures such as eutrophication and decreases in density of herbivorous fishes due to fishing pressure can alter competition between corals and algae in ways that favor algal community growth (Mumby et al. 2006; Hughes et al. 2007; Karcher et al. 2020). Understanding how communities growing over dead coral substrate influence coral reef carbonate budgets is crucial to predict whether these ecosystems will be able to maintain net CaCO_3 accretion under future environmental change.

Here, we used state-of-the-art incubation technology (Coral In-Situ Metabolism and Energetics; CISME) (Murphy et al. 2012; www.cisme-instruments.com) to perform in situ measurements of net calcification–dissolution and net photosynthesis–respiration by live corals and communities growing over dead coral substrate. The experiments were conducted in October 2018 in waters near Lizard Island, in the northern section of the Great Barrier Reef, where the coral reef ecosystem was impacted by two tropical cyclones, in 2014 and in 2015, and by two severe bleaching events, in 2016 and in 2017. These disturbances resulted in decreases in live coral cover (McMahon et al. 2019) and a shift to a benthic community dominated by algal turf (Pisapia et al. 2019). Our measurements show that dead coral substrate communities may play a larger role in daily net calcification cycles on coral reefs than previously thought.

Methods

Study site and experimental design

In situ net calcification and net photosynthesis as well as respiration and dark calcification or dissolution were measured between October 15 and October 31, 2018 at Loomis Reef ($14^\circ 41' \text{S}$, $145^\circ 27' \text{E}$) near Lizard Island, Great Barrier Reef (Fig. 1). Lizard Island is a continental granite island located 30 km off mainland Australia. The Lizard Island group refers to the main granite island and three nearby smaller islands, Palfrey, South Island and Bird. All islands are national parks and the surrounding waters are part of the Great Barrier Reef Marine Park.

Thirty-minute incubations in either blacked-out conditions to simulate the darkness of night (respiration and net dark calcification or dissolution) or under artificial lighting at $800 \mu\text{Eins m}^{-2} \text{ s}^{-1}$ (net photosynthesis and light enhanced net calcification rates) were conducted using two CISME diver-portable underwater respirometers. The CISME respirometer is designed to nondestructively measure coral metabolism in situ

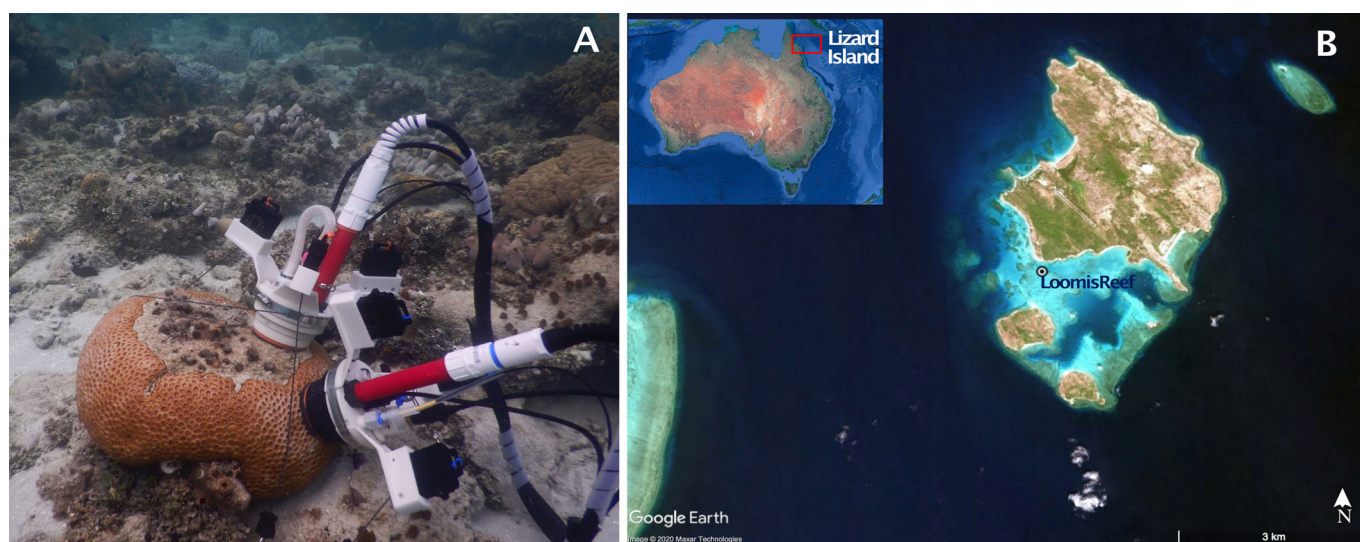


Fig. 1. (A) Photograph showing experimental setup with two CISME respirometers co-deployed on a coral colony (in this case, *Favia favus*). (B) Lizard Island group with inset showing location on the northern Great Barrier Reef.

(Dellisanti et al. 2020). The system is composed of two main parts: An electronics housing and the flow head, which are connected by electrical cables. The electronics housing contains the processor, memory, battery and a wireless network card that allows connection to an external tablet with the software that controls the system. The flow head contains the pH, dissolved oxygen, and temperature sensors, as well as a recirculation pump and a LED illumination array. The front end of the head forms a small chamber (24.5 cm² area and 69 mL volume) and a neoprene seal on the exterior provides attachment to the substrate. The pump recirculates incubation seawater at 1 L min⁻¹ from the incubation chamber past the sensors and through a removable sample loop, then back to the incubation chamber. The sample loop holds 18.6 mL of incubation fluid which can be used to withdraw samples for posterior analysis of total alkalinity to estimate calcification rates.

The CISME respirometers were deployed either on live coral colonies or on communities growing over dead coral substrate (Fig. 1A). There was an acclimation period of approximately 10 min before each experimental run. Temperature, pH, and dissolved oxygen concentration were recorded in the CISME respirometers every 2 s during the incubation. At the beginning of each deployment, discrete seawater samples were taken with glass water bottles for salinity and initial total alkalinity measurements; the CISME respirometer sample loop was retrieved at the end of each incubation for final total alkalinity measurements. Differences in total alkalinity were used to calculate calcification or carbonate dissolution rates and the CISME respirometer data output were used to calculate rates of respiration and net photosynthesis. Metabolic rates are presented per unit surface area. The dark measurements were performed as a proxy for nighttime hours since logistical constraints prevented us from making measurements at night. However, it is possible that factors such as circadian rhythms

and prior light exposure could influence metabolic rates and affect the results.

Measurements focused on the reef-building coral, *Symphyllia recta*. A few measurements were also made on *Goniastrea favulus* and *Favia favus*. All three species have non-perforate skeletons which means that the polyps enclosed within the CISME respirometer incubation area have minimal physiological interchange with the surrounding polyps. Net calcification and net photosynthesis as well as respiration and dark calcification or dissolution measurements from *G. favulus* and *F. favus* were consistent with the results described here for *S. recta* (see SI, Figs. S1 and S2). We selected coral colonies with both living and dead surface area (Fig. 1A) to compare photosynthesis–respiration and calcification–dissolution rates for both substrate types. In order to preserve coral health, multiple measurements were not taken on the same spot of any coral colony. Further, since each measurement was made with an independent CISME respirometer and measurements were not always made simultaneously on the same coral head, we treated the results from each incubation independently.

We did not explicitly characterize the biological community growing over dead coral substrate in our study. Visual assessments indicate that they were composed by a mixed algae assemblage (Fig. S4), including turf algae and carbonate sediments, which are typical of the epilithic algal matrix on reefs at Lizard Island and the Great Barrier Reef (Klumpp and McKinnon 1992; Diaz-Pulido and McCook 2004; Kramer et al. 2012), and more generally on coral reefs (Connell et al. 2014).

Carbonate chemistry measurements

Discrete samples of seawater for total alkalinity titrations were immediately returned to a shore-based laboratory, filtered

(0.45 μm), and kept in the dark until analysis on a Metrohm Titrand automatic titrator within 24 h after sample collection. Pre-standardized 0.01 mol L⁻¹ hydrochloric acid (HCl) was used for the titration. Instrument precision on $n = 97$ replicates of Certified Reference Material Batch 175 (provided by A. Dickson) distributed over 14 d of measurements was 4.90 $\mu\text{mol kg}^{-1}$ (1 SD). The average measured value of the 97 replicates (2224.76 $\mu\text{mol kg}^{-1}$) was within 0.25 $\mu\text{mol kg}^{-1}$ of the known value for Certified Reference Material Batch 175 (2224.53 $\mu\text{mol kg}^{-1}$).

Measurements of pH were performed by the CISME respirometer using a Durafet III combination electrode (Martz et al. 2010; Bresnahan et al. 2021). All pH were measured and reported on the total scale at in situ temperature. CISME respirometer pH probes were calibrated against a discrete sample taken from an intercalibration bath and measured via spectrophotometry following best practices (Dickson et al. 2007) using purified meta-cresol purple dye obtained from R. Byrne's laboratory (Liu et al. 2011) on an automated system based on the design described in (Carter et al. 2013), but instead using a MMS-UVVIS spectrophotometer with comparable performance (Takeshita et al. 2020).

All carbonate chemistry calculations were performed using pH measurements from the CISME respirometer and total alkalinity from the discrete samples as inputs into the seacarb package (Gattuso et al. 2019) in R (v. 4.0.3). Nutrient concentrations were not measured and were assumed to be zero in all calculations.

Calculations

Net calcification and dissolution rates were determined with the total alkalinity anomaly technique whereby the molar ratio of total alkalinity consumption to carbonate production is assumed to be 2 : 1 (Smith and Key 1975). Net calcification (or dissolution) was calculated as:

$$\text{Net calcification} = -\frac{1\rho V\Delta TA}{2A\tau} \quad (1)$$

where ρ is the seawater density (kg m^{-3}), V is the water volume inside the CISME respirometer and detachable loop (87.6 mL), A is the surface area covered by the CISME respirometer (24.5 cm^2), ΔTA is the final minus initial total alkalinity ($\mu\text{mol kg}^{-1}$), and τ is the time length of incubation (~ 30 min).

Net photosynthesis (or respiration) rates were calculated in a two-step process. First, we calculated the net photosynthesis (or respiration) based on continuous measurements of dissolved oxygen. We multiplied this estimate by the calculated metabolic quotients (*see below*) to estimate the net photosynthesis (or respiration) rates based on carbon units. Dissolved oxygen-based photosynthesis (or respiration) rates were calculated as:

$$\text{Net photosynthesis}_{\text{O}_2} = \frac{\rho V}{A} \hat{\beta}_{\text{O}_2} \quad (2)$$

where $\hat{\beta}_{\text{O}_2}$ is the slope of a linear regression of dissolved oxygen vs. time during the incubation. Finally, our calculation of carbon-based net photosynthesis (or respiration) was:

$$\text{Net photosynthesis} = \text{Net photosynthesis}_{\text{O}_2} \times Q \quad (3)$$

where Q is the metabolic quotient, or ratio of dissolved inorganic carbon (DIC) uptake to dissolved oxygen (O_2) production ($-\Delta\text{DIC}/\Delta\text{O}_2$). Dissolved inorganic carbon was calculated with the seacarb package in R (v. 4.0.3), using pH and temperature measurements from the CISME respirometer alongside total alkalinity and salinity measurements from discrete samples. Metabolic quotients for each incubation were determined by inverting Eq. 9 in Barnes (1983) to solve for Q . To match the continuous pH and dissolved oxygen measurements with the discrete initial and final total alkalinity measurements, we bin-averaged the first and last minute of continuous pH and dissolved oxygen measurements. To test the sensitivity of our results to our bin width, we repeated the analysis with bin widths of 30 s for the initial and final bins, and then with bin widths of 2 min for the initial and final bins. Both resulted in negligible change to the results suggesting that the choice of 1-min cutoff bins did not affect our calculations of the metabolic quotient.

Details of standard error estimations on our estimates of net calcification–dissolution and net photosynthesis–respiration are available in the SI.

Statistical tests

We tested for differences in metabolic variables (net calcification or dissolution, net photosynthesis or respiration, and the metabolic quotient) between the live coral and dead coral substrate communities in both light and dark conditions using Student's t -tests with a significance level of $\alpha = 0.05$. In total, we conducted six tests (*metabolic variable* \times *light level*). Test results are reported as *dead coral substrate* – *coral* such that the t -statistic is positive when the dead coral substrate group mean is greater than the live coral group mean and vice versa. We also subjected all six *metabolic rate* \times *light level* comparisons to Wilcoxon rank sum tests, also with a significance threshold of $\alpha = 0.05$. We compared the results from our t -tests and corresponding Wilcoxon rank sum tests to determine if any of the results were sensitive to assumptions of normality. There were no cases among the six *metabolic rate* \times *light level* groupings where the statistical significance of a test result changed between the t -test and corresponding Wilcoxon rank sum test, indicating that our reported t -test results are robust to assumptions of normality. As such, we only report the results from our t -tests.

In situ environmental conditions during incubations

The chemistry of the surrounded seawater was relatively stable in the course of the study. Seawater salinity fluctuated slightly between 35.2 and 35.6 and temperature ranged from

26.72°C to 29.22°C. The seawater total alkalinity concentration ranged between 2265.29 and 2299.10 $\mu\text{mol kg}^{-1}$.

Results

Daytime calcification rates of the dead coral substrate communities were similar to those from live corals (Fig. 2). Daytime calcification rates of live corals ranged between 3.52 and 8.68 $\text{mmol CaCO}_3 \text{ m}^{-2} \text{ h}^{-1}$ (mean = 5.75, SD = 1.74, $n = 7$), and between 1.21 and 8.89 $\text{mmol CaCO}_3 \text{ m}^{-2} \text{ h}^{-1}$ (mean = 4.07, SD = 2.46, $n = 7$) for the dead coral substrate communities. This difference was not statistically significant ($t = -1.4686$, $df = 10.787$, $p = 0.1705$). However, in dark conditions, live corals maintained positive calcification rates, while the dead coral substrate communities were net dissolving (Fig. 2). Dark calcification rates of live corals varied from 0.52 to 3.55 $\text{mmol CaCO}_3 \text{ m}^{-2} \text{ h}^{-1}$ (mean = 2.25, SD = 0.83, $n = 11$), while the dead coral substrate communities were always net dissolving with rates varying between -3.36 and $-0.39 \text{ mmol CaCO}_3 \text{ m}^{-2} \text{ h}^{-1}$ (mean = -2.09 , SD = 0.81, $n = 11$). The dark calcification rates of live corals were significantly greater than those of dead coral substrate communities ($t = -12.361$, $df = 19.98$, $p < 0.001$).

The metabolic quotient is the ratio of dissolved inorganic carbon consumption (or production) to oxygen production

(or consumption) during metabolic activities. In light conditions, it reflects the combined activities of gross photosynthesis and community respiration. In dark conditions, it reflects changes in dissolved inorganic carbon and dissolved oxygen due to community respiration. For consistency, we always present the net metabolic quotient as changes in dissolved inorganic carbon divided by changes in dissolved oxygen. The metabolic quotient was calculated by combining total alkalinity measurements made on our discrete samples, with our continuous measurements of pH and dissolved oxygen (Barnes 1983).

The metabolic quotient in the light was higher in the dead coral substrate communities compared to live corals (Fig. 3). Light metabolic quotient values in dead coral substrate communities varied between 1.53 and 2.00 (mean = 1.75, SD = 0.15, $n = 7$), whereas for the live corals values ranged from 0.40 to 1.05 (mean = 0.83, SD = 0.21, $n = 7$). This difference was statistically significant ($t = 9.2602$, $df = 10.81$, $p < 0.001$). The dark metabolic quotient for dead coral substrate communities ranged between 0.21 and 1.05 (mean = 0.71, SD = 0.25, $n = 11$), while for live corals it ranged from 0.91 to 1.30 (mean = 1.02, SD = 0.12, $n = 11$). This difference was also statistically significant ($t = -3.5456$, $df = 14.174$, $p < 0.01$). Some of the low values in the dark for dead coral substrate communities could be due to limits in the analytical error of total alkalinity when the changes were small.

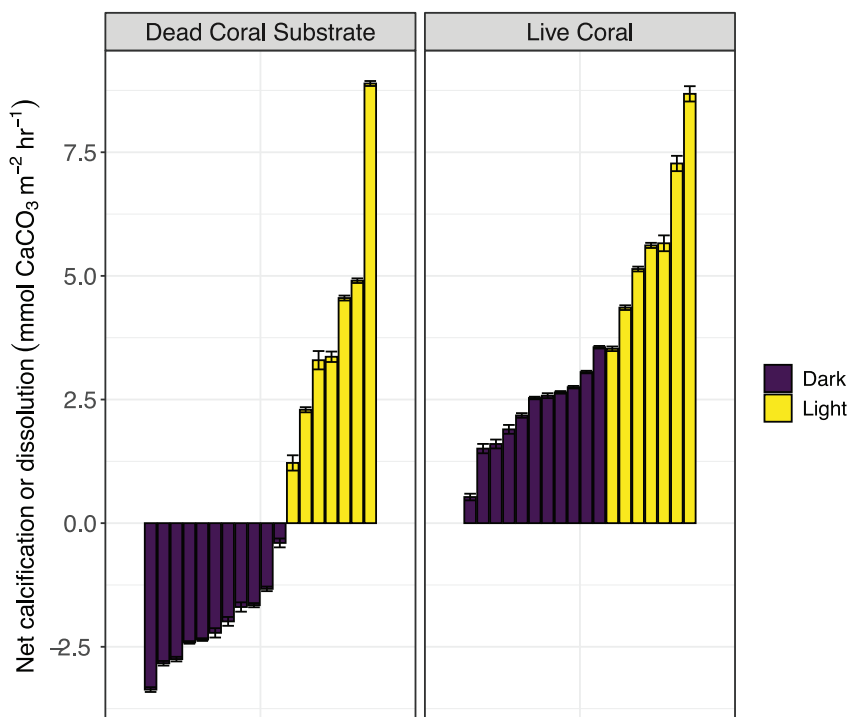


Fig. 2. Net calcification or dissolution rates for each CISME respirometer experimental replicate over living and dead *Symphyllia recta*. The left panel shows measurements for the dead coral substrate and the right panel shows measurements for the live coral. Each bar represents an individual CISME respirometer run. Yellow bars show light measurements and purple bars show dark measurements. The error bars show the standard error for each calculated net calcification rate (seeSI for calculation).

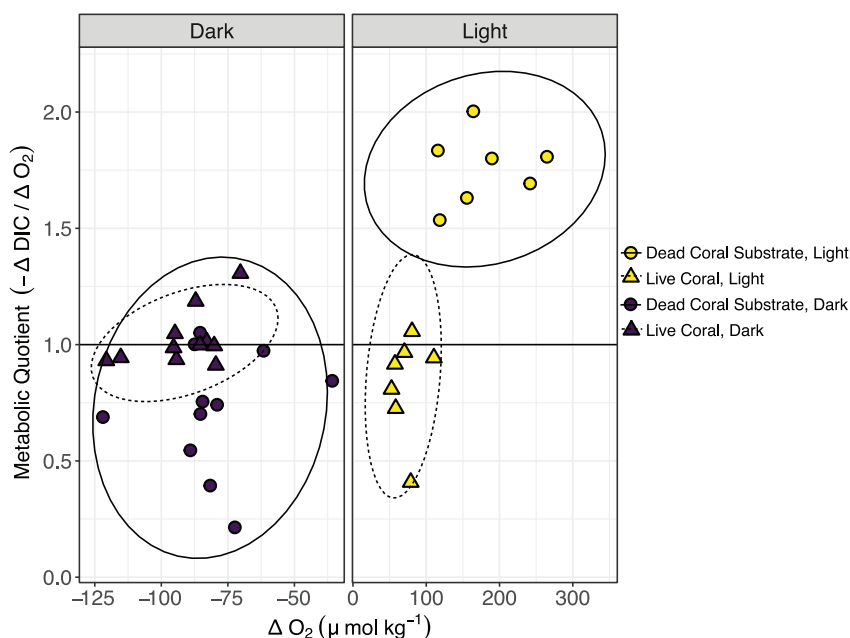


Fig. 3. Metabolic quotient (ratio of changes in dissolved inorganic carbon to changes in dissolved oxygen) for CISME respirometer measurements made in dark (left panel) and light (right panel) on live *Symphyllia recta* (triangles) and dead *S. recta* (circles). Each point represents an individual CISME respirometer measurement. 95% confidence ellipses are shown for the live coral (dashed) and dead coral substrate communities (solid).

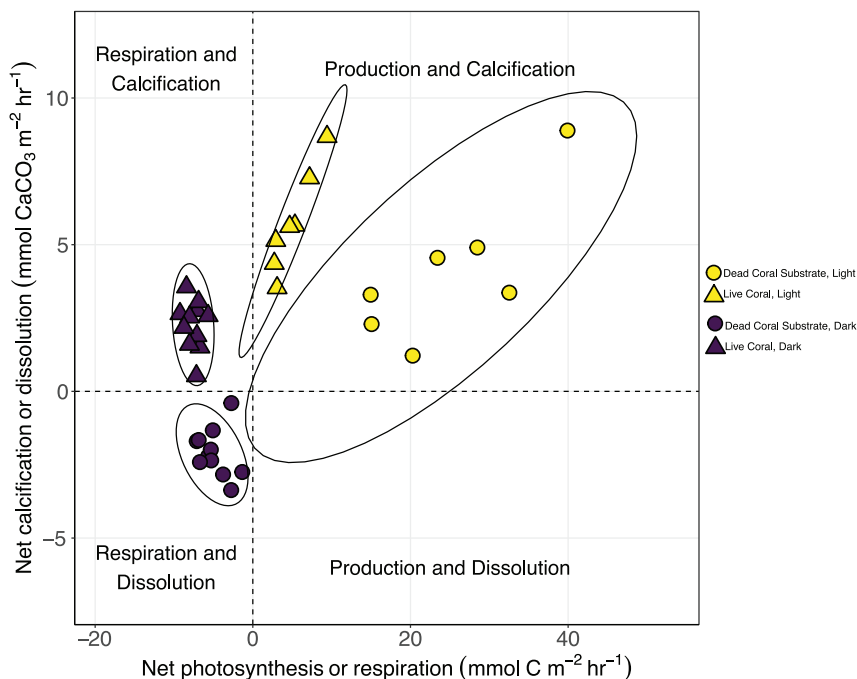


Fig. 4. Net photosynthetic or respiration rates and net calcification or dissolution rates for each CISME respirometer experimental replicate over live coral (*Symphyllia recta*) and dead coral substrate community. Each circle/triangle represents an individual CISME respirometer replicate. The circles show measurements from the dead coral substrate communities and the triangles show measurements from the live corals. Yellow circle/triangle shows deployment with light and purple circle/triangles show deployment performed in the dark. All light experiments were performed at $800 \mu\text{Eins m}^{-2} \text{s}^{-1}$. 95% confidence ellipses are shown for the live coral and dead coral substrate community.

Light net photosynthesis of live corals varied from 2.72 to 9.41 mmol C m⁻² h⁻¹ (mean = 5.04, SD = 2.50, *n* = 7) and light net photosynthesis of the dead coral substrate communities varied between 14.94 and 39.91 mmol C m⁻² h⁻¹ (mean = 24.95, SD = 9.27, *n* = 7). Net photosynthesis was significantly higher for the dead coral substrate communities when compared to live corals ($t = 5.4817$, $df = 6.837$, $p < 0.001$) (Fig. 4). Dark respiration rates varied from -9.23 to -5.66 mmol C m⁻² h⁻¹ (mean = -7.54, SD = 1.03, *n* = 11) for live corals and between -7.11 and -1.34 mmol C m⁻² h⁻¹ (mean = -4.78, SD = 1.90, *n* = 11) for the dead coral substrate communities. Respiration rates were significantly greater for the live corals than for the dead coral substrate communities ($t = 4.2248$, $df = 15.488$, $p < 0.001$).

Figure 4 shows that live coral and dead coral substrate separate into different quadrants of the net calcification/dissolution vs. net photosynthesis/respiration diagram. While there is a large range of values within each group, the sign of each group is clear: all light treatments resulted in net photosynthesis, all dark treatments resulted in respiration, and only the dark dead coral substrate treatment resulted in both respiration and dissolution.

Discussion

This study provides new data that suggest the dynamics of calcium carbonate precipitation and dissolution on dead coral surfaces may be as complicated as the dynamics in living corals. The unexpectedly high calcification rates observed for dead coral substrate communities indicate that coral reef calcification dynamics are not solely attributed to hard corals and coralline algae. While it has been assumed that corals dominate the calcification signal of coral reef ecosystems (Odum and Odum 1955; Kinsey 1985), we provide evidence for a paradigm shift for coral reef calcification at the level of dead coral assemblages. Since light calcification did not significantly differ between corals and dead coral substrate, as reefs shift away from coral-dominated states toward algal-covered states, our results demonstrate that rates of daytime net calcification, as inferred from measurements of total alkalinity anomalies in the water column, may not change while coral cover and structural complexity declines.

Mixed algal assemblages grow quickly on the carbonate substrate of dead coral and rubble after disturbance events (Adey 1998; Diaz-Pulido and McCook 2004; Diaz-Pulido et al. 2009). They are composed of taxonomically-diverse algae and cyanobacteria, including coralline algae, which are important non-coral contributors to net calcification in the Great Barrier Reef (Adey 1998). In fact, some algal assemblages have been reported as being mainly composed of coralline algae (Blockley and Chapman 2008; Connell et al. 2014), but calcifying algae did not dominate the dead coral surfaces in our study. Mixed algal assemblages provide habitat for an abundant and diverse community of small invertebrates (Klumpp

et al. 1988; Smith et al. 2001; Kramer et al. 2012). On Lizard Island, cryptozoa that occupy algal assemblages are dominated by several calcifiers and bioeroders, including crustaceans, polychaetes and gastropods (Kramer et al. 2014). Little is known about the contribution of these small but highly abundant groups to net carbonate production in coral reef ecosystems. While they may be adding to the net calcification within the algal communities growing over dead coral substrate at Lizard Island, their direct magnitude of calcification is likely to be minimal (Wolfe et al. 2020) compared to the overall contribution of calcifying algae and nearby living coral.

In addition to biological processes (biomineralization), carbonate precipitation in the ocean can be induced abiotically (spontaneous precipitation) if carbonate mineral saturation states are sufficiently elevated and nucleation sites exist. This limit for abiotic precipitation has been estimated to be at $\Omega_{\text{Calcite}} > 20$ (Morse and He 1993; Sun et al. 2015), which corresponds to $\Omega_{\text{Aragonite}} > 14.5$ at the temperature and salinity conditions during our measurements. The $\Omega_{\text{Aragonite}}$ calculated for the dead coral substrate communities at the end of each light incubation varied between 4.90 and 6.86, while for live corals, it varied between 2.26 and 2.68. While the $\Omega_{\text{Aragonite}}$ in the dead coral substrate incubations greatly exceeded that of the overlying reef water ($\Omega_{\text{Aragonite}} = 2.96\text{--}4.75$), these values did not reach the $\Omega_{\text{Aragonite}} > 14.5$ threshold necessary to facilitate abiotic precipitation of CaCO₃ in the water column. Although the bulk water in the CISME respirometer was not sufficient for abiotic precipitation to occur, the dead coral substrate communities may provide microhabitats with higher $\Omega_{\text{Aragonite}}$ conditions due to their high photosynthetic rates and complex microstructure (Fig. 4). It is possible that carbonate precipitation could have been ongoing in microenvironments within the dead coral substrate where localized supersaturation might exceed a critical level due to photosynthesis by the algal community or the microorganisms inhabiting these microenvironments. In nature, microorganisms are able to induce carbonate precipitation by a wide range of metabolic processes. The most common in the marine environment is photosynthesis by cyanobacteria (Zhu and Dittrich 2016). When these metabolic processes take place in relatively closed systems such as cavities where fluid exchange is low they affect water chemistry favoring localized precipitation or dissolution, which could occur relatively far from the inducing community (Webb 2001).

An important difference between the dead coral substrate communities and live corals was that the corals calcified in the dark, whereas calcium carbonate substrate or particles associated with the dead coral communities dissolved in the dark. The bulk seawater $\Omega_{\text{Aragonite}}$ was well above 1 (2.59–3.61) when dissolution was observed. The fact that dissolution processes are taking place in this supersaturated seawater may be another indication that microenvironments within the reef matrix are playing an important role in the calcification and dissolution pathways observed in the dead coral substrate,

similar to what happens in reef sediments (Kessler et al. 2020). In these microenvironments, microbial remineralization of organic matter may produce dissolution due to CO₂ production, even when the overlying seawater is supersaturated with respect to carbonate minerals (Andersson and Gledhill 2013).

Communities associated with reef framework have been previously identified as one of the primary calcifying components of a coral reef in microcosm experiments (Small and Adey 2001). Assemblages of turf algae, along with foraminifera and crustose corallines, accounted for nearly 30% of the total calcification. The abiotic formation of micritic aragonite crystals beneath the mixed algal assemblages were suggested to be the main driver of the measured calcification. In our study, the main driver for carbonate precipitation in the dead coral substrate was not determined, but our observations are consistent with microenvironment induced precipitation and dissolution.

The higher biomass-specific primary productivity of dead coral substrate communities over live corals observed on Lizard Island suggests that shifts in benthic community composition on coral reefs due to climate change may lead to increases in ecosystem productivity. Dead coral heads may be colonized by thick mats of microalgae that have high biomass-specific rates of photosynthesis and primary productivity (Heil et al. 2004). Algal turfs, which also typically colonize dead coral surfaces, are also characterized by high productivity despite their low biomass (Carpenter 1985, 1986). This may be explained as a life-history strategy of microalgae and algal turfs where success is a result of growing slightly faster than herbivores can consume them (Steneck and Dethier 1994; Hatcher 1997). The extent to which shifts in community composition influence primary productivity is site-specific, as productivity among algal assemblages is highly variable and can increase with intense grazing (Steneck and Dethier 1994), due to factors such as increased N₂ fixation, regeneration of nutrients and light effects due to canopy removal (Williams and Carpenter 1990). Furthermore, the production rates of coral reef substrates are not solely reliant on community composition but are a function of other factors such as light, temperature, nutrient availability, sedimentation and flow (Long et al. 2013; Koweek et al. 2015; Takeshita et al. 2018). In a changing ocean, enhanced productivity of algal assemblages may benefit many herbivores (Cheal et al. 2008, 2010; Wilson et al. 2009; Russ et al. 2015), but keeping their height low is important for the successful recruitment of corals (Roth et al. 2018), and thus reef recovery post-disturbance (Graham et al. 2015; Wolfe et al. 2020). It is important to note that while dead coral substrate communities may have high levels of production and calcification, they will not serve the same ecosystem functions as corals which provide the complex calcium carbonate habitat critical to reef formation.

Lastly, the calculated metabolic quotients in this study were highly variable, especially when comparing live corals

and dead coral substrate communities. These data indicate that assuming community metabolic quotients of one in the absence of a better estimate, which has long been a common practice in the scientific community, may lead to overestimation or underestimation of primary productivity in units of carbon when converting between measurements of dissolved inorganic carbon and dissolved oxygen (Kinsey 1985). This practice may result in erroneous assumptions especially in those studies where productivity between different benthic groups are compared, and more studies are needed to help constrain the metabolic quotient on coral reefs.

In summary, our results provide evidence that dead coral substrate communities may contribute substantially to the carbonate budgets of disturbed coral reefs by unexpectedly high calcification rates during daytime and dissolution at night. A shift is needed in our interpretation of net coral reef calcification as inferred from measurements of total alkalinity anomalies, and the link between live coral cover, and reef accretion and function (Roff 2020). Given that coral reef calcium carbonate dynamics are not solely attributed to hard corals and coralline algae, this new evidence questions the assumption that percent coral cover should be directly linked to ecosystem calcification rates. While it is likely that dead coral substrate communities have always contributed to reef carbonate budgets, their increased benthic cover after disturbance events implies that their contributions to daily calcification/dissolution cycling may become increasingly prominent in future coral reef carbonate budgets.

Our data suggest that shifts in benthic community composition on coral reefs may not necessarily affect the amount of gross calcification occurring in the coral reef community, but by strongly affecting whether the carbonate mineral produced in the daytime survives nighttime dissolution, shifts in benthic community composition may strongly affect the amount of net calcification. Our results indicate that coral reefs may shift from slow, long-term accumulators of CaCO₃ to become daily cyclers of calcium carbonate with little or no long-term accretion. If reefs transition from long-term accumulators of CaCO₃ into high frequency carbonate cyclers, they may tip into states of net erosion by failing to produce enough carbonate minerals to offset physical erosion. In conjunction with projected sea level rise, analysis of these carbonate mass budget terms should give an estimate of how long the physical structure of eroding coral reefs may be expected to persist.

Data availability statement

All data and code necessary to reproduce the results of this paper are publicly available at: <http://doi.org/10.5281/zenodo.4527823>.

References

Adey, W. H. 1998. Review-CORAL reefs: Algal structured and mediated ecosystems in shallow, turbulent, alkaline waters.

- J. Phycol. **34**: 393–406. doi:[10.1046/j.1529-8817.1998.340393.x](https://doi.org/10.1046/j.1529-8817.1998.340393.x)
- Albright, R., et al. 2018. Carbon dioxide addition to coral reef waters suppresses net community calcification. *Nature* **555**: 516–519. doi:[10.1038/nature25968](https://doi.org/10.1038/nature25968)
- Andersson, A. J., and D. Gledhill. 2013. Ocean acidification and coral reefs: Effects on breakdown, dissolution, and net ecosystem calcification. *Ann. Rev. Mar. Sci.* **5**: 321–348. doi:[10.1146/annurev-marine-121211-172241](https://doi.org/10.1146/annurev-marine-121211-172241)
- Barnes, D. J. 1983. Profiling coral reef productivity and calcification using pH and oxygen electrodes. *J. Exp. Mar. Biol. Ecol.* **66**: 149–161. doi:[10.1016/0022-0981\(83\)90036-9](https://doi.org/10.1016/0022-0981(83)90036-9)
- Blockley, D. J., and M. G. Chapman. 2008. Exposure of seawalls to waves within an urban estuary: Effects on intertidal assemblages. *Austral Ecol.* **33**: 168–183. doi:[10.1111/j.1442-9993.2007.01805.x](https://doi.org/10.1111/j.1442-9993.2007.01805.x)
- Bresnahan, P. J., and others. 2021. Autonomous in situ calibration of ion-sensitive field effect transistor pH sensors. *Limnol. Oceanogr.: Methods* **19**: 132–144. doi:[10.1002/lom3.10410](https://doi.org/10.1002/lom3.10410)
- Bruno, J. F., and E. R. Selig. 2007. Regional decline of coral cover in the Indo-Pacific: timing, extent, and subregional comparisons. *PLoS One* **2**: e711. doi:[10.1371/journal.pone.0000711](https://doi.org/10.1371/journal.pone.0000711)
- Carpenter, R. C. 1985. Relationships between primary production and ii radiance in coral reef algal communities: Production of reef algae. *Limnol. Oceanogr.* **30**: 784–793. doi:[10.4319/lo.1985.30.4.0784](https://doi.org/10.4319/lo.1985.30.4.0784)
- Carpenter, R. C. 1986. Partitioning herbivory and its effects on coral reef algal communities. *Ecol. Monogr.* **56**: 345–364. doi:[10.2307/1942551](https://doi.org/10.2307/1942551)
- Carter, B. R., J. A. Radich, H. L. Doyle, and A. G. Dickson. 2013. An automated system for spectrophotometric seawater pH measurements: Automated spectrophotometric pH measurement. *Limnol. Oceanogr.: Methods* **11**: 16–27. doi:[10.4319/lom.2013.11.16](https://doi.org/10.4319/lom.2013.11.16)
- Cheal, A. J., S. K. Wilson, M. J. Emslie, A. M. Dolman, and H. Sweatman. 2008. Responses of reef fish communities to coral declines on the Great Barrier Reef. *Mar. Ecol. Prog. Ser.* **372**: 211–223. doi:[10.3354/meps07708](https://doi.org/10.3354/meps07708)
- Cheal, A. J., M. A. MacNeil, E. Cripps, M. J. Emslie, M. Jonker, B. Schaffelke, and H. Sweatman. 2010. Coral-macroalgal phase shifts or reef resilience: Links with diversity and functional roles of herbivorous fishes on the Great Barrier Reef. *Coral Reefs* **29**: 1005–1015. doi:[10.1007/s00338-010-0661-y](https://doi.org/10.1007/s00338-010-0661-y)
- Clements, C. S., D. B. Rasher, A. S. Hoey, V. E. Bonito, and M. E. Hay. 2018. Spatial and temporal limits of coral-macroalgal competition: the negative impacts of macroalgal density, proximity, and history of contact. *Mar. Ecol. Prog. Ser.* **586**: 11–20. doi:[10.3354/meps12410](https://doi.org/10.3354/meps12410)
- Connell, S. D., M. S. Foster, and L. Airoidi. 2014. What are algal turfs? Towards a better description of turfs. *Mar. Ecol. Prog. Ser.* **495**: 299–307. doi:[10.3354/meps10513](https://doi.org/10.3354/meps10513)
- Courtney, T. A., and A. J. Andersson. 2019. Evaluating measurements of coral reef net ecosystem calcification rates. *Coral Reefs* **38**: 997–1006. doi:[10.1007/s00338-019-01828-2](https://doi.org/10.1007/s00338-019-01828-2)
- Cyronak, T., I. R. Santos, A. McMahon, and B. D. Eyre. 2013. Carbon cycling hysteresis in permeable carbonate sands over a diel cycle: Implications for ocean acidification. *Limnol. Oceanogr.* **58**: 131–143. doi:[10.4319/lo.2013.58.1.0131](https://doi.org/10.4319/lo.2013.58.1.0131)
- DeCarlo, T. M., A. L. Cohen, G. T. F. Wong, F.-K. Shiah, S. J. Lentz, K. A. Davis, K. E. F. Shamberger, and P. Lohmann. 2017. Community production modulates coral reef pH and the sensitivity of ecosystem calcification to ocean acidification: Production modulates pH and calcification. *J. Geophys. Res. C: Oceans* **122**: 745–761. doi:[10.1002/2016JC012326](https://doi.org/10.1002/2016JC012326)
- Dellisanti, W., R. H. L. Tsang, P. Ang, J. Wu, M. L. Wells, and L. L. Chan. 2020. A diver-portable Respirometry system for in-situ short-term measurements of coral metabolic health and rates of calcification. *Front. Mar. Sci.* **7**: 932. doi:[10.3389/fmars.2020.571451](https://doi.org/10.3389/fmars.2020.571451)
- Diaz-Pulido, G., and L. J. McCook. 2004. Effects of live coral, epilithic algal communities and substrate type on algal recruitment. *Coral Reefs* **23**: 225–233.
- Diaz-Pulido, G., and others. 2009. Doom and boom on a resilient reef: Climate change, algal overgrowth and coral recovery. *PLoS One* **4**: e5239. doi:[10.1371/journal.pone.0005239](https://doi.org/10.1371/journal.pone.0005239)
- Dickson, A. G., C. L. Sabine, and J. R. Christian. 2007. Guide to best practices for ocean CO₂ measurements. North Pacific Marine Science Organization.
- Eyre, B. D., T. Cyronak, P. Drupp, E. H. De Carlo, J. P. Sachs, and A. J. Andersson. 2018. Coral reefs will transition to net dissolving before end of century. *Science* **359**: 908–911. doi:[10.1126/science.aao1118](https://doi.org/10.1126/science.aao1118)
- Gardner, T. A., I. M. Côté, J. A. Gill, A. Grant, and A. R. Watkinson. 2003. Long-term region-wide declines in Caribbean corals. *Science* **301**: 958–960. doi:[10.1126/science.1086050](https://doi.org/10.1126/science.1086050)
- Gattuso, J.-P., J.-M. Epitalon, H. Lavigne, and J. Orr. 2019. seacarb: Seawater carbonate chemistry. R package version 3.2. 12.
- Graham, N. A. J., S. Jennings, M. A. MacNeil, D. Mouillot, and S. K. Wilson. 2015. Predicting climate-driven regime shifts versus rebound potential in coral reefs. *Nature* **518**: 94–97. doi:[10.1038/nature14140](https://doi.org/10.1038/nature14140)
- Harris, J. L. 2015. The ecology of turf algae on coral reefs. UC San Diego.
- Hatcher, B. G. 1997. Organic production and decomposition. In: Birkeland C (ed) *Life and death of coral reefs*. Chapman & Hall, New York, pp 140–174.
- Heil, C. A., K. Chaston, A. Jones, P. Bird, B. Longstaff, S. Costanzo, and W. C. Dennison. 2004. Benthic microalgae in coral reef sediments of the southern Great Barrier Reef, Australia. *Coral Reefs* **23**: 336–343.

- Hughes, T. P., et al. 2007. Phase shifts, herbivory, and the resilience of coral reefs to climate change. *Curr. Biol.* **17**: 360–365. doi:[10.1016/j.cub.2006.12.049](https://doi.org/10.1016/j.cub.2006.12.049)
- Karcher, D. B., and others. 2020. Nitrogen eutrophication particularly promotes turf algae in coral reefs of the Central Red Sea. *PeerJ* **8**: e8737. doi:[10.7717/peerj.8737](https://doi.org/10.7717/peerj.8737)
- Kayanne, H., et al. 2005. Seasonal and bleaching-induced changes in coral reef metabolism and CO₂ flux. *Glob. Biogeochem. Cycles* **19**: GB3015. doi:[10.1029/2004GB002400](https://doi.org/10.1029/2004GB002400)
- Kessler, A. J., and others. 2020. Pore water conditions driving calcium carbonate dissolution in reef sands. *Geochim. Cosmochim. Acta* **279**: 16–28.
- Kinsey, D. W. 1985. Metabolism, calcification and carbon production: 1 systems level studies, p. 505–526. *In* C. Gabrie and B. Salvat [eds.], *Proc. 5th Int. Coral Reef Cong.*
- Klumpp, D. W., and A. D. McKinnon. 1992. Community structure, biomass and productivity of epilithic algal communities on the Great Barrier Reef: Dynamics at different spatial scales. *Mar. Ecol. Prog. Ser.* **86**: 77–89.
- Klumpp, D. W., A. D. McKinnon, and C. N. Mundy. 1988. Motile cryptofauna of a coral reef: Abundance, distribution and trophic potential. *Mar. Ecol. Prog. Ser.* **45**: 95–108. doi:[10.3354/MEPS045095](https://doi.org/10.3354/MEPS045095)
- Koweek, D., R. B. Dunbar, J. S. Rogers, G. J. Williams, N. Price, D. Mucciarone, and L. Teneva. 2015. Environmental and ecological controls of coral community metabolism on Palmyra Atoll. *Coral Reefs* **34**: 339–351. doi:[10.1007/s00338-014-1217-3](https://doi.org/10.1007/s00338-014-1217-3)
- Kramer, M. J., D. R. Bellwood, and O. Bellwood. 2012. Cryptofauna of the epilithic algal matrix on an inshore coral reef, Great Barrier Reef. *Coral Reefs* **31**: 1007–1015. doi:[10.1007/s00338-012-0924-x](https://doi.org/10.1007/s00338-012-0924-x)
- Kramer, M. J., D. R. Bellwood, and O. Bellwood. 2014. Benthic Crustacea on coral reefs: A quantitative survey. *Mar. Ecol. Prog. Ser.* **511**: 105–116. doi:[10.3354/meps10953](https://doi.org/10.3354/meps10953)
- Liu, X., M. C. Patsavas, and R. H. Byrne. 2011. Purification and characterization of meta-cresol purple for spectrophotometric seawater pH measurements. *Environ. Sci. Technol.* **45**: 4862–4868. doi:[10.1021/es200665d](https://doi.org/10.1021/es200665d)
- Long, M. H., P. Berg, D. de Beer, and J. C. Ziemann. 2013. In situ coral reef oxygen metabolism: An eddy correlation study. *PLoS One* **8**: e58581. doi:[10.1371/journal.pone.0058581](https://doi.org/10.1371/journal.pone.0058581)
- Martz, T. R., J. G. Connery, and K. S. Johnson. 2010. Testing the Honeywell Durafet® for seawater pH applications: Durafet seawater evaluation. *Limnol. Oceanogr.: Methods* **8**: 172–184. doi:[10.4319/lom.2010.8.172](https://doi.org/10.4319/lom.2010.8.172)
- McMahon, A., I. R. Santos, K. G. Schulz, A. Scott, J. Silverman, K. L. Davis, and D. T. Maher. 2019. Coral reef calcification and production after the 2016 bleaching event at Lizard Island, Great Barrier Reef. *J. Geophys. Res. C: Oceans* **124**: 4003–4016. doi:[10.1029/2018JC014698](https://doi.org/10.1029/2018JC014698)
- Morse, J. W., and S. He. 1993. Influences of T, S and PCO₂ on the pseudo-homogeneous precipitation of CaCO₃ from seawater: Implications for whiting formation. *Mar. Chem.* **41**: 291–297. doi:[10.1016/0304-4203\(93\)90261-L](https://doi.org/10.1016/0304-4203(93)90261-L)
- Mumby, P. J., and others. 2006. Fishing, trophic cascades, and the process of grazing on coral reefs. *Science* **311**: 98–101. doi:[10.1126/science.1121129](https://doi.org/10.1126/science.1121129)
- Murphy, B. A., C. H. Mazel, R. Whitehead, and A. M. Szmant. 2012. CISME: A self-contained diver portable metabolism and energetics system, p. 1–7. *In* *Proceeding of the Oceans*. Hampton Roads, VA. doi:[10.1109/OCEANS.2012.6405075](https://doi.org/10.1109/OCEANS.2012.6405075)
- Odum, H. T., and E. P. Odum. 1955. Trophic Structure and Productivity of a Windward Coral Reef Community on Eniwetok Atoll. *Ecol. Monogr.* **25**: 291–320. doi:[10.2307/1943285](https://doi.org/10.2307/1943285)
- Page, H. N., T. A. Courtney, A. Collins, E. H. De Carlo, and A. J. Andersson. 2017. Net Community Metabolism and Seawater Carbonate Chemistry Scale Non-intuitively with Coral Cover. *Frontiers in Marine Science* **4**: 161. doi:[10.3389/fmars.2017.00161](https://doi.org/10.3389/fmars.2017.00161)
- Pisapia, C., E. J. Hochberg, and R. Carpenter. 2019. Multi-decadal change in reef-scale production and calcification associated with recent disturbances on a Lizard Island reef flat. *Front. Mar. Sci.* **6**: 575. doi:[10.3389/fmars.2019.00575](https://doi.org/10.3389/fmars.2019.00575)
- Roff, G. 2020. Reef accretion and coral growth rates are decoupled in Holocene reef frameworks. *Mar. Geol.* **419**: 106065. doi:[10.1016/j.margeo.2019.106065](https://doi.org/10.1016/j.margeo.2019.106065)
- Rogers, C. S., and J. Miller. 2006. Permanent ‘phase shifts’ or reversible declines in coral cover? Lack of recovery of two coral reefs in St. John, US Virgin Islands. *Mar. Ecol. Prog. Ser.* **306**: 103–114. doi:[10.3354/meps306103](https://doi.org/10.3354/meps306103)
- Roth, F., F. Saalman, T. Thomson, D. J. Coker, R. Villalobos, B. H. Jones, C. Wild, and S. Carvalho. 2018. Coral reef degradation affects the potential for reef recovery after disturbance. *Mar. Environ. Res.* **142**: 48–58. doi:[10.1016/j.marenvres.2018.09.022](https://doi.org/10.1016/j.marenvres.2018.09.022)
- Russ, G. R., S.-L. A. Questel, J. R. Rizzari, and A. C. Alcala. 2015. The parrotfish–coral relationship: Refuting the ubiquity of a prevailing paradigm. *Mar. Biol.* **162**: 2029–2045. doi:[10.1007/s00227-015-2728-3](https://doi.org/10.1007/s00227-015-2728-3)
- Small, A. M., and W. H. Adey. 2001. Reef corals, zooxanthellae and free-living algae: A microcosm study that demonstrates synergy between calcification and primary production. *Ecol. Eng.* **16**: 443–457. doi:[10.1016/S0925-8574\(00\)00066-5](https://doi.org/10.1016/S0925-8574(00)00066-5)
- Smith, S. V., and G. S. Key. 1975. Carbon dioxide and metabolism in marine environments. *Limnol. Oceanogr.* **20**: 493–495. doi:[10.4319/lo.1975.20.3.0493](https://doi.org/10.4319/lo.1975.20.3.0493)
- Smith, J., C. Smith, and C. Hunter. 2001. An experimental analysis of the effects of herbivory and nutrient enrichment on benthic community dynamics on a Hawaiian reef. *Coral Reefs* **19**: 332–342. doi:[10.1007/s003380000124](https://doi.org/10.1007/s003380000124)
- Steneck, R. S., and M. N. Dethier. 1994. A functional group approach to the structure of algal-dominated communities. *Oikos* **69**: 476–498. doi:[10.2307/3545860](https://doi.org/10.2307/3545860)

- Sun, W., S. Jayaraman, W. Chen, K. A. Persson, and G. Ceder. 2015. Nucleation of metastable aragonite CaCO₃ in seawater. *Proc. Natl. Acad. Sci. USA* **112**: 3199–3204. doi:[10.1073/pnas.1423898112](https://doi.org/10.1073/pnas.1423898112)
- Swierts, T., and M. J. Vermeij. 2016. Competitive interactions between corals and turf algae depend on coral colony form. *PeerJ* **4**: e1984. doi:[10.7717/peerj.1984](https://doi.org/10.7717/peerj.1984)
- Takeshita, Y., T. Cyronak, T. R. Martz, T. Kindeberg, and A. J. Andersson. 2018. Coral reef carbonate chemistry variability at different functional scales. *Front. Mar. Sci.* **5**: 175. doi:[10.3389/fmars.2018.00175](https://doi.org/10.3389/fmars.2018.00175)
- Takeshita, Y., K. S. Johnson, L. J. Coletti, H. W. Jannasch, P. M. Walz, and J. K. Warren. 2020. Assessment of pH dependent errors in spectrophotometric pH measurements of seawater. *Mar. Chem.* **223**: 103801. doi:[10.1016/j.marchem.2020.103801](https://doi.org/10.1016/j.marchem.2020.103801)
- Webb, G. E. 2001. Biologically Induced Carbonate Precipitation in Reefs through Time. In: Stanley G.D. (eds) *The History and Sedimentology of Ancient Reef Systems*. Topics in Geobiology, vol 17. Springer, Boston, MA. doi:[10.1007/978-1-4615-1219-6_5](https://doi.org/10.1007/978-1-4615-1219-6_5)
- Williams, S. L., and R. C. Carpenter. 1990. Photosynthesis/ photon flux density relationships among components of CORAL reef algal TURFS1. *J. Phycol.* **26**: 36–40. doi:[10.1111/j.0022-3646.1990.00036.x](https://doi.org/10.1111/j.0022-3646.1990.00036.x)
- Wilson, S. K., A. M. Dolman, A. J. Cheal, M. J. Emslie, M. S. Pratchett, and H. P. A. Sweatman. 2009. Maintenance of fish diversity on disturbed coral reefs. *Coral Reefs* **28**: 3–14. doi:[10.1007/s00338-008-0431-2](https://doi.org/10.1007/s00338-008-0431-2)
- Wolfe, K., and others. 2020. Priority species to support the functional integrity of coral reefs. *Oceanogr. Mar. Biol.: Annu. Rev.* **58**: 185.
- Zhu, T., and M. Dittrich. 2016. Carbonate precipitation through microbial activities in natural environment, and their potential in biotechnology: A Review. *Front. Bioeng. Biotechnol.* **4**: 4. doi:[10.3389/fbioe.2016.00004](https://doi.org/10.3389/fbioe.2016.00004)

Acknowledgments

This study was supported by the Carnegie Institution for Science endowment, and, in part, by the California Academy of Sciences ‘Hope for Reefs’ Initiative. The study was partially supported by the Lizard Island Postdoctoral Fellowship awarded to TC funded by the Yulgilbar Foundation and Australian Museum’s Lizard Island Research Station. Work was conducted under Great Barrier Reef Marine Park Authority Permit G17/39550.1. The authors are grateful to the staff at the Lizard Island Research Station, Anne Hoggett and Lyle Vail in particular, for the logistical support.

Conflict of Interest

None declared.

Submitted 04 June 2020

Revised 07 October 2020

Accepted 04 February 2021

Associate editor: Steeve Comeau